Clinical Pharmacokinetics (2022) 61:997–1012
https://doi.org/10.1007/s40262-022-01121-6

ORIGINAL RESEARCH ARTICLE

Determining the Effects of Chronic Kidney Disease on Organic Anion Transporter1/3 Activity Through Physiologically Based Pharmacokinetic Modeling

Samuel Dubinsky[1] · Paul Malik[1] · Dagmar M. Hajducek[1] · Andrea Edginton[1]

Accepted: 6 March 2022 / Published online: 5 May 2022

Abstract

Background and Objective The renal excretion of drugs via organic anion transporters 1 and 3 (OAT1/3) is significantly decreased in patients with renal impairment. This study uses physiologically based pharmacokinetic models to quantify the reduction in OAT1/3-mediated secretion of drugs throughout varying stages of chronic kidney disease.

Methods Physiologically based pharmacokinetic models were constructed for four OAT1/3 substrates in healthy individuals: acyclovir, meropenem, furosemide, and ciprofloxacin. Observed data from drug–drug interaction studies with probenecid, a potent OAT1/3 inhibitor, were used to parameterize the contribution of OAT1/3 to the renal elimination of each drug. The models were then translated to patients with chronic kidney disease by accounting for changes in glomerular filtration rate, kidney volume, renal blood flow, plasma protein binding, and hematocrit. Additionally, a relationship was derived between the estimated glomerular filtration rate and the reduction in OAT1/3-mediated secretion of drugs based on the renal extraction ratios of p-aminohippuric acid in patients with varying degrees of renal impairment. The relationship was evaluated in silico by evaluating the predictive performance of each final model in describing the pharmacokinetics (PK) of drugs across stages of chronic kidney disease.

Results OAT1/3-mediated renal excretion of drugs was found to be decreased by 27–49%, 50–68%, and 70–96% in stage 3, stage 4, and stage 5 of chronic kidney disease, respectively. In support of the parameterization, physiologically based pharmacokinetic models of four OAT1/3 substrates were able to adequately characterize the PK in patients with different degrees of renal impairment. Total exposure after intravenous administration was predicted within a 1.5-fold error and 85% of the observed data points fell within a 1.5-fold prediction error. The models modestly under-predicted plasma concentrations in patients with end-stage renal disease undergoing intermittent hemodialysis. However, results should be interpreted with caution because of the limited number of molecules analyzed and the sparse sampling in observed chronic kidney disease pharmacokinetic studies.

Conclusions A quantitative understanding of the reduction in OAT1/3-mediated excretion of drugs in differing stages of renal impairment will contribute to better predictive accuracy for physiologically based pharmacokinetic models in drug development, assisting with clinical trial planning and potentially sparing this population from unnecessary toxic exposures.

1 Introduction

Chronic kidney disease (CKD) affects nearly 10% of the global population [1]. Chronic kidney disease is defined by a reduction in kidney function as approximated by the glomerular filtration rate (GFR) below 60 mL/min/1.73 m^2 for 3 months or more [2]. Several equations to approximate GFR are used in clinical practice such as the Cockcroft–Gault, Modification of Diet in Renal Disease, or the CKD Epidemiology Collaboration equations [2]. Stages of CKD are classified by the degree of renal impairment, with stage 3, stage 4, and stage 5 defined by estimated GFR values of 59–30, 29–15, and < 15 mL/min/1.73 m^2, respectively [2]

Patients with CKD may take more than 12 different prescription drugs per day to reduce morbidity and mortality associated with the disease [3]. It is a clinical challenge to ensure safe and effective dosing for each of these medications in patients with renal impairment because CKD affects many aspects of pharmacokinetics (PK) and drug disposition. Most intuitively, renal elimination pathways are

✉ Andrea Edginton
aedginto@uwaterloo.ca

[1] School of Pharmacy, University of Waterloo, Waterloo, ON, Canada

Key Points

Physiologically based pharmacokinetic models were successfully developed to describe how organic anion transporter 1 and 3 (OAT1/3) activity may be compromised across the stages of chronic kidney disease and to predict the pharmacokinetics (PK) of drugs that undergo OAT1/3-mediated renal excretion.

Quantifying the relationship between the p-aminohippuric acid extraction ratio and the estimated glomerular filtration rate demonstrated that reductions in OAT-mediated renal excretion may occur disproportionately to that of glomerular filtration as chronic kidney disease progresses.

The proposed workflow adequately predicts the intravenous PK and renal elimination of four OAT substrates in patients with chronic kidney disease but may modestly over-predict renal elimination in patients undergoing intermittent hemodialysis.

compromised. About one-third of the most prescribed drugs in the USA undergo renal elimination and 90% of these are actively secreted by the kidney [4]. While passive filtration of drugs into urine declines directly in proportion to the GFR, the progressive decline in secretory function in each stage of CKD remains poorly understood.

There are two common groups of transporters by which drugs can be actively secreted from the interstitial space of the nephron across the renal epithelium and into the urine. Cations may be taken up by organic cation transporter 2 and secreted into urine by P-glycoprotein and/or the multidrug and toxin extrusion transporters (MATE1, MATE2K) [5]. Anions may be taken up by organic anion transporters 1 and 3 (OAT1/3) and secreted into the urine by the multidrug resistance proteins 1–4 [5]. A recent review summarizes evidence that the activities of apical efflux transporters are largely preserved in CKD [5]. The renal clearances of drugs that are substrates for organic cation transporter 2 tend to decline in parallel with GFR, suggesting that the activity of renal organic cation transporters may not be significantly compromised by uremia [6, 7]. However, there is convincing evidence that the activities or expression of renal OAT transporters may be significantly compromised in renal impairment, with this inhibition driven by high levels of circulating uremic toxins [5, 8, 9]. The progressive decline in renal clearance for most OAT1/3 substrates is more severe than the decline in GFR [10, 11].

In this work, a parameterization for the relative activity of OAT1/3 transporters across various stages of renal impairment is developed and evaluated using a mechanism-based modeling approach. Physiologically based pharmacokinetic (PBPK) models represent drug absorption, distribution, metabolism, and excretion within virtual individuals according to the actual mechanisms responsible, as far as can be feasibly identified. This exercise leverages recent advancements in PBPK modeling in patients with CKD that quantify the systemic impact of the disease on parameters related to renal, hemodynamic, and gastrointestinal physiology [7]. Building on this foundation, we developed PBPK models for four drugs that are OAT substrates (acyclovir, meropenem, furosemide, ciprofloxacin) with the overall objective of using a physiological model to understand how OAT1/3 activity may be compromised in patients with varying degrees of renal impairment and evaluated their predictive accuracy when the parameterization for OAT activity is applied.

2 Methods

2.1 Software

All PBPK modeling was carried out using PK-Sim version 9.1 as part of the Open Systems Pharmacology suite (www.open-systems-pharmacology.org). Parameter sets for healthy adults and aged persons in European and white American populations have been described previously [12, 13]. Scientific data to inform the individual and population-level parameter changes in CKD were applied using MATLAB R2021a (Mathworks, Natick, MA, USA) as published previously [7]. A noncompartmental analysis of observed PK datasets was conducted with the PKNCA package in R where necessary.

2.2 PBPK Models for Healthy Adults

PBPK models were constructed to mechanistically represent the PK of four drugs that are substrates of OAT1/3 in healthy adults. A detailed report of model development and verification for each molecule in healthy adults is available in the Electronic Supplementary Material (ESM). The final parameters for each molecule are presented in Table 1.

Briefly, each model in healthy adults was developed by collecting and appraising the physicochemicl properties of each molecule from the literature. Organ-specific partition coefficients were calculated with the PK-Sim standard, Schmitt, or the Rodgers and Rowland algorithms [29–31]. Information regarding the expression and localization of renal transporters was extracted from Ivanyuk et al. and previously published PBPK models [15, 25]. It was assumed that basolateral uptake into the renal epithelium by OAT1 and OAT3 occurs via one generic OAT transporter within the models as the processes are not uniquely identifiable.

Previous PBPK models for drugs with active tubular secretion often simplified the two processes of basolateral influx and apical efflux with 'global' renal drug transporters to represent the net flux into urine. Such assumptions were largely owing to the absence of in vitro and in vivo data to parameterize each process separately [7, 11, 32]. In this work, uptake via OAT transport was mathematically identified by optimizing against a drug–drug interaction (DDI) study with one arm where OAT activity was strongly inhibited by probenecid and one control arm. The PBPK model for probenecid was downloaded from the Open Systems Pharmacology repository and can be found at: https://github.com/Open-Systems-Pharmacology/Probenecid-Model [15]. Probenecid is a competitive inhibitor of OAT with an inhibition constant (K_I) of 5.41 µM; previous validation of this inhibition constant for prediction of the furosemide-probenecid DDI has been published [15]. In the DDI simulation of probenecid and the OAT substrates, the apparent Michaelis–Menten constant for OAT transport ($K_{M,app}$) was calculated as (Eq. 1):

$$Km_{app} = Km \times \left(1 + \frac{I}{K_I}\right), \quad (1)$$

where I represents the concentration of the competitive inhibitor, probenecid [15].

Incorporating empirical data derived from probenecid-DDI PK studies follows a "middle-out" approach, which

Table 1 Physiologically based pharmacokinetic model parameters

Parameter	Ciprofloxacin	Furosemide	Meropenem	Acyclovir
Fraction unbound in plasma (f_u)	0.67 [14]	0.022 [15]	0.98 [16, 17]	0.85 [18]
Lipophilicity (log$P$)	0.95 [14]	− 0.24	− 1.21[a] [− 1.21 to − 1.21]	− 0.69[a] [− 0.69 to − 0.69]
Molecular weight (g/mol)	331.30 [14]	330.74	383.46 [17, 19]	225.21 [18]
Effective molecular weight (g/mol) accounting for halogens	314.30	330.74	383.46	225.21
Fraction excreted in urine (fe; %)	61.2 ± 7.2 [20]	74 ± 7 [15]	79 ± 2 [21]	86.2 ± 11.4 [22]
Contribution of TS of CL_R[e] (%)	73	98	96	74
Partition coefficient algorithm	PK-Sim Standard	Schmitt	Rodgers and Rowland	Rodgers and Rowland
Cell permeability algorithm	PK-Sim Standard	Charge-dependent Schmitt	Charge-dependent Schmitt	Charge-dependent Schmitt
GFR fraction	1.0	1.0	1.0	1.0
OAT concentration (µM)	0.0917[b] [15]	0.0917[b] [15]	0.0917[b] [15]	0.0917[b] [15]
OAT V_{max} (µM/min)	5.96[a] (M/min) [5.60–6.30]	754.40 [15]	1262.57[a] [1248.49–1268.14]	25.75[a] (mM/min) [25.70–26.19]
OAT Km (µM)	70 [23]	21.50 [15]	847 [24]	342.30 [23]
Apical transporter type	TS[c]	MRP4 [15]	TS[c]	MATE [25]
Apical transporter concentration (µM)	1.0[b]	0.02[b] [26, 27]	1.0[b]	1.0[b]
Apical transporter V_{max} (µM/min)	58.39[a] [55.45–61.62]	163.09 [15]	116.11[a] [115.67–117.16]	0.99[a] (mM/min) [0.98–0.99]
Apical transporter Km (µM)	1000	27.96 [15]	770 [28]	3480 [23]
Metabolizing enzyme	CYP 1A2[b]	UGT 1A9[b] [15]	Renal DHP-1[b] [21]	CMMG[d]
Metabolizing enzyme concentration (µM)	1.8	0.197 [15]	1.0	1.0
Metabolizing enzyme specific clearance (L/µmol/min)	0.027[a] [0.027–0.027]	187.53 [15]	89.21[a] [88.99–89.90]	0.031[a] [0.031–0.031

[a]Parameters optimized from their literature values

[b]Relative expression in human organs extracted from the PK-Sim Gene Database for Humans

[c]TS; generic apical transporter on the apical side of kidney cells

[d]CMMG; assumed first-order metabolism within the liver

[e]Percentage of tubular secretion of renal clearance was calculated as $(CL_R - f_u \times GFR)/CL_R$

implements an in vitro understanding of the PK (bottom-up) with observed clinical data (top-down) [33–35]. Although this modeling strategy differs slightly from "traditional" PBPK model development, it provides the most mechanistically accurate approach in the absence of a proper method to scale in vitro data for OAT transport to in vivo.

For uncertain parameters, numerical optimization was performed using the parameter identification tool in PK-Sim. A Monte Carlo method was used to search the parameter space for the optimal solution that minimized the sum of the squared error on the simulated vs observed drug concentrations and fractions excreted to urine. Multiple optimization runs (6–10) were performed to confirm identifiability of a unique solution.

The models that were optimized using mean individuals were then expanded to simulate the pharmacokinetics in virtual populations for model verification. Datasets for model verification are presented in the ESM. One hundred individuals were generated for each virtual population. Patient demographics were set according to those reported in each observed study population being simulated. User-defined variability was assigned to the renal transporter concentrations with a normal distribution and a coefficient of variation of 20% [7, 36]. Verification was assessed using the average fold error (AFE) (Eq. 2) and absolute average fold error (AAFE) (Eq. 3) for each simulation. Acceptance was confirmed if the AFE was < 30% (0.7–1.3) and the AAFE was ≤ 2. For data sets including individual patient samples, inter-individual variability in the population simulation was accepted if 85–95% of observed concentrations fell within the 90th prediction interval.

$$\mathrm{AFE} = 10^{\frac{1}{N}\sum_i \log\left(\frac{\mathrm{predicted}_i}{\mathrm{observed}_i}\right)}, \tag{2}$$

$$\mathrm{AAFE} = 10^{\frac{1}{N}\sum_i \left|\log\left(\frac{\mathrm{predicted}_i}{\mathrm{observed}_i}\right)\right|}, \tag{3}$$

where $\mathrm{predicted}_i$ and $\mathrm{observed}_i$ correspond to predicted and observed plasma concentrations respectively.

2.3 PBPK Models for CKD

Final population models for healthy adults were carried forward for evaluation in CKD with modifications to account for the systemic changes in whole-body anatomy and physiology that occur throughout the course of the disease such as GFR, kidney volume, renal perfusion, hematocrit, and plasma protein concentrations. The methodology and evaluation of this modeling strategy have been published previously [7]. Additionally, nonrenal clearance (CL_{NR}) was scaled for various stages of CKD to account for inhibition or downregulation of liver enzymes due to chronic uremia throughout disease progression as outlined in the corresponding section [35]. Utilizing the CKD-PBPK modeling approach, we produced several PBPK models across stages 3–5 of CKD to evaluate the proposed parameterization for OAT activity in CKD.

Predictive accuracy for the extrapolation to CKD was assessed by a limit of a 1.5-fold error (0.67–1.5) when comparing simulated exposures to observed data from the literature. Exposure was quantified as the area under the concentration–curve extrapolated to infinity (AUC_∞). If AUC_∞ was not reported within the study, AUC_∞ was calculated by noncompartmental analysis. Additionally, predicted vs observed half-lives were compared. The limit of a 1.5-fold error for each PK parameter was used as the threshold for acceptable performance when extrapolating to vulnerable and diverse populations based on previous criteria used in recent years [11, 37].

Additionally, model performance against the conventional AUC scaling method was also explored. Scaling AUC_∞ from healthy individuals was conducted using:

$$\mathrm{AUC}_{\mathrm{CKD}} = \frac{\mathrm{BW}_{\mathrm{CKD}}}{\mathrm{BW}_{\mathrm{Healthy}}} \cdot \mathrm{AUC}_{\mathrm{Healthy}} \div \left[\mathrm{fe} \cdot \frac{\mathrm{GFR}_{\mathrm{CKD}}}{\mathrm{GFR}_{\mathrm{Healthy}}} + (1 - \mathrm{fe})\right], \tag{4}$$

where AUC is the area under the concentration–time curve extrapolated to infinity for CKD and healthy individuals respectively, BW is body weight, GFR is glomerular filtration rate, and fe is the fraction excreted to urine unchanged after an intravenous dose. Within this assessment, patients undergoing dialysis were assumed to have a GFR of 5 mL/min/1.73 m^2.

2.4 OAT Parameterization

The utility of *p*-aminohippuric acid (PAH) as a diagnostic indicator of renal plasma flow and tubular excretion was first discovered in the 1940s by Smith et al. [38]. Based on its physicochemical properties, PAH has since become recognized as a prototypical OAT substrate and has helped to define the OAT pathway of several drugs [39–42]. Numerous publications have since quantified the activity of OAT excretion in various stages of CKD by comparing the renal extraction ratio of PAH (EPAH%) to eGFR [42–47]. Individual patient data was extracted, and several exploratory analyses were conducted to describe the relationship between EPAH and eGFR, including the logarithmic of EPAH, LASSO regression, and polynomial function. Ultimately, a Weibull function utilizing Poisson weighting and setting the intercept equivalent to zero was used to convey this relationship. Weighting of observed EPAH values was conducted to characterize the EPAH in patients with severe renal impairment. The resulting EPAH% vs eGFR relationship is presented in Fig. 1.

The final function of EPAH (y) and eGFR (x) was given by (Eq. 5):

$$\text{EPAH}(\%) = \left(1 - e^{\left(-\left(\frac{\text{eGFR}}{43.9}\right)^{0.9}\right)}\right) \times 100\%. \quad (5)$$

This parameterization describes how OAT mediated secretory function declines through various stages of CKD due to a combination of transporter down-regulation and competitive OAT inhibition from uremic solutes [5, 8, 9].

2.5 Non-renal Clearance in CKD

Evolving data suggest that CKD reduces CL_{NR} through various mechanisms [48–50]. Work conducted by Sayama et al. quantified the reduction in CL_{NR} for several metabolic pathways [35]. The mean relative percentage (RP%) of CL_{NR} was 69% for moderate CKD (eGFR: 30–59 mL/min/1.73 m^2) and 64% for severe CKD (eGFR: 15–29 mL/min/1.73 m^2) compared to healthy individuals [35]. The mean RP was used to scale CL_{NR} in our PBPK simulations across the stages of CKD. It was assumed that the mean RP of CL_{NR} for stage 5 CKD (GFR < 15 mL/min/1.73 m^2) was consistent with severe CKD (RP = 64%).

2.6 Sensitivity Analysis

A local sensitivity analysis was performed to test the importance of OAT activity for DDI potential in healthy adults and each stage of CKD. Simulations were built for mean male individuals at stages 3, 4, and 5 (ESRD) and healthy conditions. All virtual subjects received a standard therapeutic dose of each drug (i.e., 400 mg intravenously for ciprofloxacin, 40 mg intravenously for furosemide). Organic anion transporter activity in each scenario was varied by 10% and the relative changes in AUC_∞ were reported as sensitivity coefficients. The sensitivity coefficient (S^p) for the effect of the parameter (p) on the PK output (PK) was calculated as the average of:

$$S^p = \left|\frac{\text{PK}(p + 0.1 \times p) - \text{PK}(p)}{\text{PK}(p)}\right| \times \frac{100\%}{10\%}. \quad (6)$$

Therefore, a sensitivity coefficient of 1 means that a 10% change in the parameter value caused a ± 10% change in the PK output, and a sensitivity coefficient of 0.1 means that a 10% change in the parameter value caused a ± 1% change in the PK output.

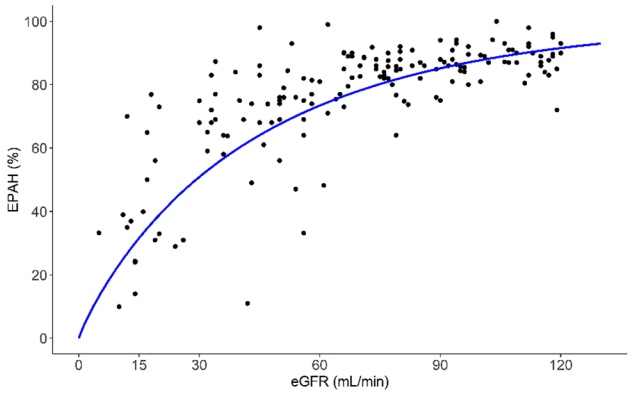

Fig. 1 Parameterization of organic anion transporter 1 and 3 functionality across varying stages of chronic kidney disease. Data investigating the relationship between the p-aminohippuric acid extraction ratio (EPAH) and the estimated glomerular filtration rate (eGFR) were extracted from several studies (black dots) [42–47]. A Weibull function (blue line) was determined to be the best representation of the relationship between EPAH and eGFR

3 Results

3.1 PBPK Models for Healthy Adults

Population PBPK models for four OAT substrate drugs were developed and verified to describe the mechanistic disposition in healthy adults with an explicit contribution of OAT characterized using DDI modeling with probenecid. Detailed reports of model development and verification of meropenem, acyclovir, and ciprofloxacin are shown in the ESM. Furosemide model development and verification was included from previous work by another group [15]. Figure 2 shows the fitted concentration vs time profiles for the DDI with probenecid for each drug.

Active tubular secretion mediated by OAT transport contributes to a significant percentage of renal clearance (CL_R) (60–98%) for each investigative drug. This PBPK-DDI modeling strategy enabled us to identify a unique solution for this process. Upon model simulation, all individual and population model simulations fell within the predefined acceptance criteria for the model fit.

3.2 PBPK Models for CKD

Parameters for virtual individuals in the healthy populations were then modified to simulate the PK of OAT substrate drugs in various stages of CKD. Parameterization for CKD included a novel quantification of OAT activity, reduction in CL_{NR}, and foundational CKD physiological scaling [7]. To assess the accuracy of this approach and success of the OAT parameterization, predictions for exposure and half-life were compared to observed data from eight clinical trials across CKD stages 3–5 (Table 2).

Mean AUC_∞ was predicted within a 1.5-fold error across all observed data sets except for two involving patients with

ESRD undergoing intermittent hemodialysis (IHD) receiving meropenem (Figs. 3, 4, 5, 6). Within these data sets, predicted AUC_{∞} was within a two-fold error of observed values. The meropenem-CKD model was able to accurately capture clearance processes in ESRD; however, it significantly underpredicted maximum concentration (C_{max}) [Fig. 6]. Of note, AUC_{∞} predictions were suitable for CKD stages 3 and 4 within the same trials. Similarly, C_{max} was underpredicted within our acyclovir-CKD model, which may have contributed to underpredictions in AUC_{∞}.

Of the remaining CKD-PBPK simulations, predicted AUC_{∞} fell within a 1.5-fold error of observed values across all stages of CKD. Additionally, seven of the 15 predictive AUC_{∞} values were within a more rigorous 1.25-fold error (Fig. 7a). Predicted elimination half-life within the CKD-PBPK simulations fell within a 1.5-fold error for 11 of the 15 simulations. Predictive accuracy for an elimination half-life resulted in an equal number of over-predictions and under-predictions.

Overall, AUC_{∞} tended to be modestly underpredicted in eight of the 15 simulations over the course of CKD progression. This trend was most notably witnessed with meropenem and acyclovir, both of which undergo large contributions of OAT-mediated clearance. This error is largely driven by an inability to accurately capture C_{max} in these simulations, but the contribution of reduced apical transporter activity is plausible.

The conventional scaling method for predicting AUC failed to meet the 1.5-fold criteria in seven of 12 empirical calculations (58%). Most notably, scaling predictions were unsuccessful in CKD stages 4 and 5. Comparisons of the conventional scaling method to observed values may be found in Fig. 7b.

Representative PK profiles with interindividual variability may be found in Figs. 3, 4, 5, 6. Overall, 85% of the simulated mean drug concentrations for CKD stages 3–5 fell within 1.5-fold of the corresponding observed drug concentrations used for model verification. Including simulations with ESRD between dialysis sessions, approximately 80%

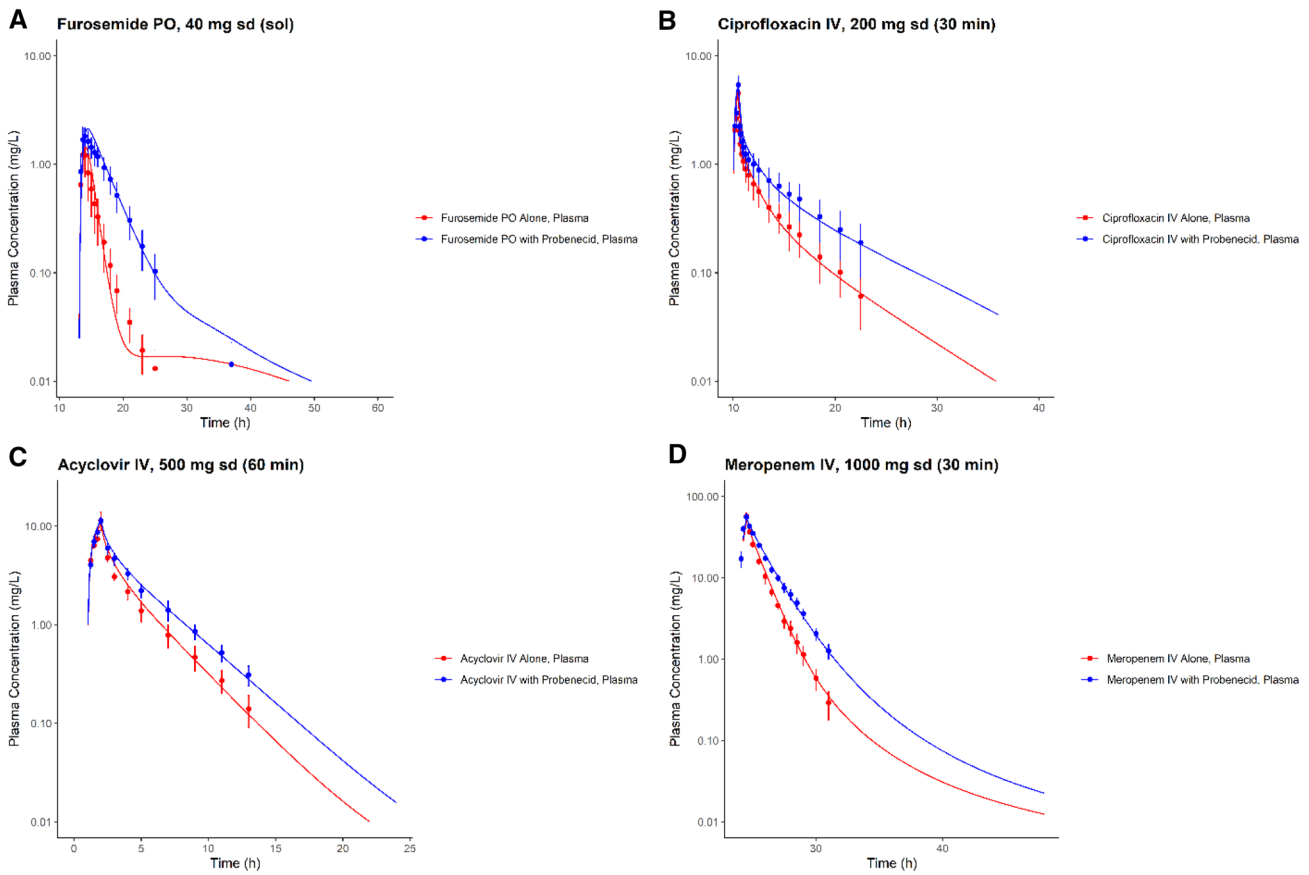

Fig. 2 Simulated physiologically based pharmacokinetic-drug–drug interaction plasma concentration–time profiles after optimization compared to observed data for **A** furosemide, **B** ciprofloxacin, **C** acyclovir, and **D** meropenem. Observed data presented as mean (circles) with standard error of the mean (error bars) for each respective study [20, 21, 51, 52]. The blue line represents the same dose of investigative drug administered after completion of probenecid dosing protocols. Details on dosing regimen and study populations are shown in each respective ESM file. *IV* intravenous, *PO* by mouth, *sd* single dose, *sol* solution

Table 2 Exposure predictions of drugs undergoing active tubular secretion via organic anion transporters in chronic kidney disease

Study	Drug	Dose (mg)	GFR (mL/min) [range]	Observed AUC (mg•h/L)	Predicted AUC (mg• h/L)	Scaled AUC (mg •h/L)	Observed *t½* (h)	Predicted *t½* (h)
Stage 3								
Drusano et al. [54]	Ciprofloxacin	200 mg IV	39.84 [13.33–56.67]	12.36	12.36	10.98	7.7 ± 1.22	8.57
Shah et al. [55]	Ciprofloxacin	400 mg IV every 12 h	44.8 [31.3–59.9]	21.5	23.22	**11.59**	5.72	**9.77**
Chimata et al. [53]	Meropenem	500 mg IV	34.13 [32–37.3]	74.6 ± 29	88.26	Healthy comparator not available	3.36 ± 1.02	2.31
Christensson et al. [56]	Meropenem	500 mg IV	34 ± 11.8	89.8 ± 17.9	89.86	82.6	2.34	2.84
Leroy et al. [57]	Meropenem	500 mg IV	50.3 ± 16.7 [30–80]	88 ± 33.9	66.35	65.81	1.93 ± 0.81	2.61
Stage 4								
Gladziwa et al. [58]	Furosemide	120 mg IV	16.7 ± 5.5 [7–27]	47.2 ± 15.6	60.05	Healthy comparator not available	4.6 ± 3	**2.81**
Christensson et al. [56]	Meropenem	500 mg IV	17 ± 8	156 ± 63.8	128.88	**99.89**	3.82	5.24
Stage 5								
Drusano et al. [54]	Ciprofloxacin	200 mg IV	IHD	15.06	20.35	17.56	8.55 ± 3.27	10.82
Shah et al. [55]	Ciprofloxacin	300 mg IV every 12 h	14.5 [4.8–24.1]	30.1	25.86	**19.18**	8.33	11.75
Rane et al. [59]	Furosemide	80 mg IV	11 ± 1	27.79	39.84	26.89	2.6	2.66
Chimata et al .[53]	Meropenem	500 mg IV	12.08 [4.3–21.5]	186.8 ± 68.5	157.25	Healthy comparator not available	5 ± 1.05	3.61
Christensson et al. [56]	Meropenem	500 mg IV	IHD	393 ± 83.8	**207.21**	**91.04**	6.81	6
Leroy et al. [57]	Meropenem	500 mg IV	12.7 ± 6.6 [2–30]	179 ± 64.1	136.38	**110.34**	5.22 ± 1.58	**7.79**
Leroy et al. [57]	Meropenem	500 mg IV	IHD	360 ± 108	**204.33**	**118.71**	9.73 ± 3.03	9.15
Laskin et al. [60]	Acyclovir	2.5 mg/kg IV	IHD	354.51[a] (µmol• h/L)	265.77[a] (µmol •h/L)	**102.50**	19.5 ± 5.9	**11.4**

Data presented as mean ± standard deviation (range)

Bolded region indicates failed predictions

AUC area under the concentration–time curve, *GFR* glomerular filtration rate, *h* hours, *IHD* intermittent hemodialysis, *IV* intravenous, *t½* half-life

[a]AUC calculated until the last sampling time due to initiation of dialysis

of simulated mean drug concentrations met the acceptance criteria (Fig. 1 of the ESM).

3.3 Sensitivity Analysis

Local sensitivity analyses for the four investigative drugs reveal the importance of OAT activity related to exposure in both healthy individuals and those across the stages of CKD (Fig. 8). Organic anion transporter *K*m and V_{max} appear to be less influential on AUC_{∞} throughout CKD progression. Based upon this analysis, patients with CKD may be less vulnerable to OAT-mediated DDIs compared with healthy adults. A recent in vivo analysis determined that PAH clearance was reduced by nearly 50% in subtotal nephrectomy rats compared with the healthy rat model in the presence of probenecid OAT-mediated inhibition [61]. Because of

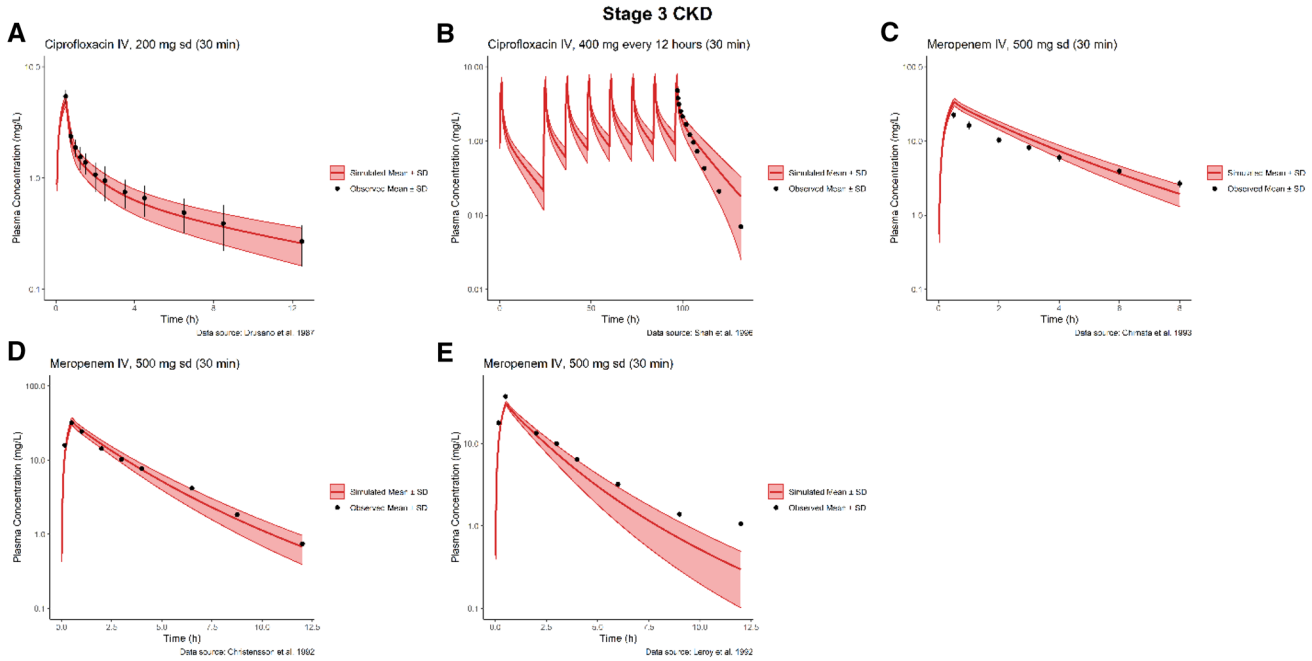

Fig. 3 Simulated chronic kidney disease-physiologically based pharmacokinetic (CKD-PBPK) plasma concentration–time profiles compared to observed data for CKD stage 3. Observed data presented as mean (circles) with standard error of the mean (error bars) for each respective study [53–57]. The red line represents the simulated mean concentration–time profile facilitated by the population CKD-PBPK models in PK-Sim, while the shaded region indicates the corresponding standard deviation (SD). Details on the dosing regimen and study populations are shown in the ESM. *IV* intravenous, *sd* single dose

OAT transporter downregulation and/or inhibition from uremic toxin accumulation, it is plausible that there are fewer available binding sites for inhibitors to occupy as CKD progresses. However, to our knowledge, there is no clinical data in humans to support this theory and further research is needed to investigate this hypothesis.

4 Discussion

In this work, we demonstrated that PBPK models for CKD populations that additionally incorporated a new parameterization for the impairment of OAT transporter secretory

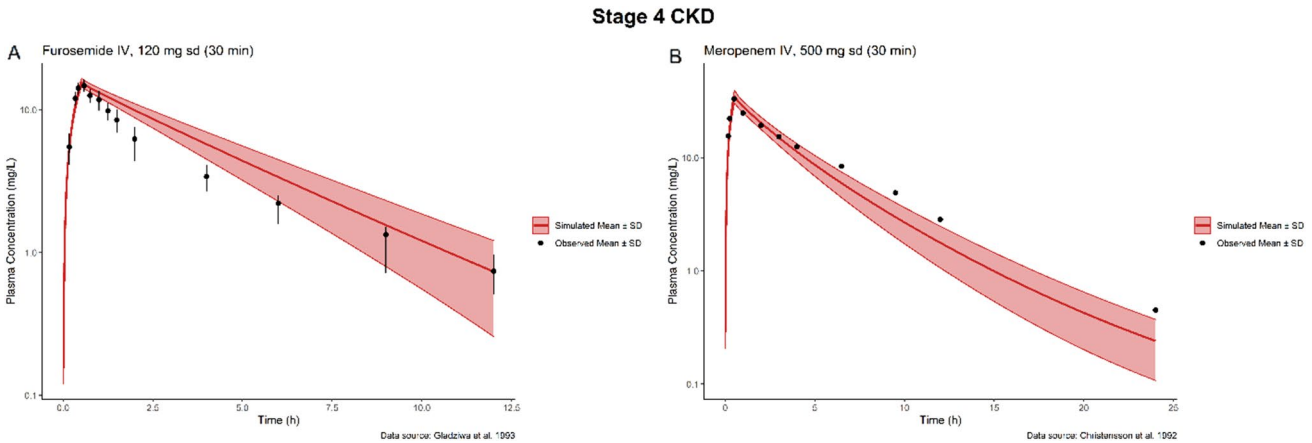

Fig. 4 Simulated chronic kidney disease-physiologically based pharmacokinetic (CKD-PBPK) plasma concentration–time profiles compared to observed data for CKD stage 4. Observed data presented as mean (circles) with standard error of the mean (error bars) for each respective study [56, 58]. The red line represents the simulated mean concentration–time profile facilitated by the population CKD-PBPK models in PK-Sim, while the shaded region indicates the corresponding standard deviation (SD). Details on the dosing regimen and study populations are shown in the ESM. *IV* intravenous, *sd* single dose

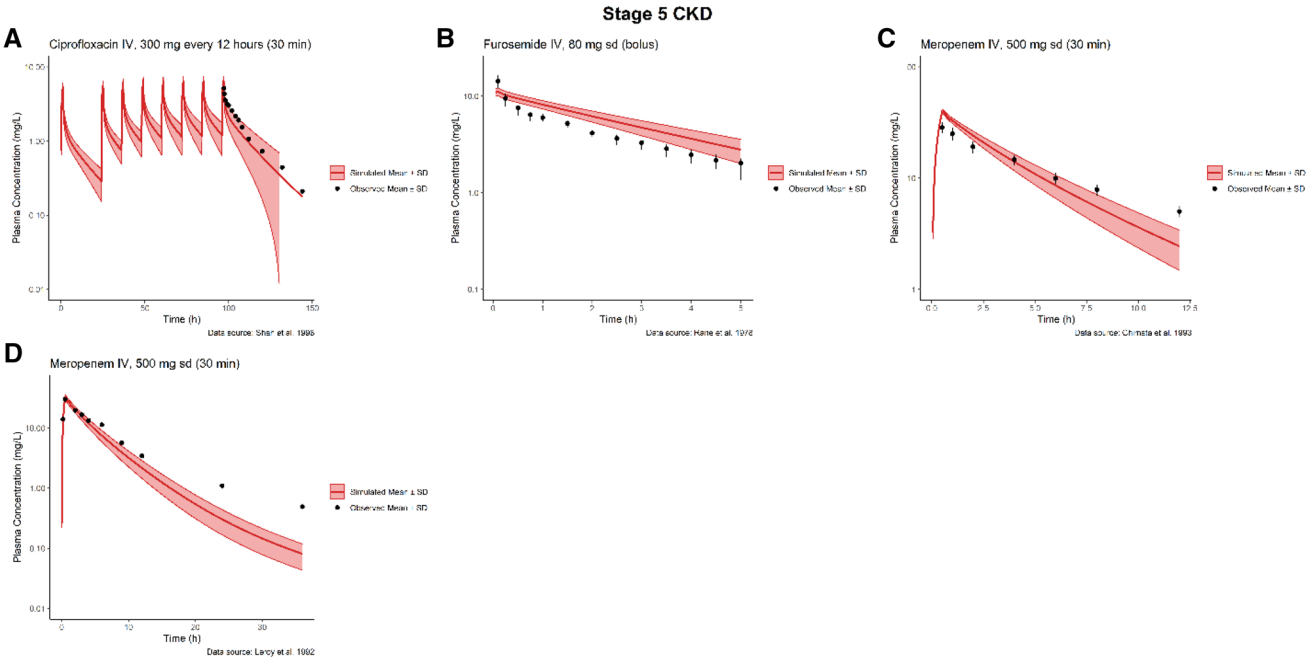

Fig. 5 Simulated chronic kidney disease-physiologically based pharmacokinetic (CKD-PBPK) plasma concentration–time profiles compared to observed data for CKD stage 5 without administration of intermittent hemodialysis. Observed data presented as mean (circles) with standard error of the mean (error bars) for each respective study [53, 54, 57, 58]. The red line represents the simulated mean concentration–time profile facilitated by the population CKD-PBPK models in PK-Sim, while the shaded region indicates the corresponding standard deviation (SD). Details on the dosing regimen and study populations are shown in the ESM. *IV* intravenous, *sd* single dose

activity adequately described the pharmacokinetics of four renally cleared OAT substrates ($fe_{urine} > 0.5$) with a high contribution of active tubular secretion (> 60% to CL_R) in patients across various stages of CKD but struggled to capture the pharmacokinetics in patients receiving IHD between dialysis sessions. Recent efforts have addressed the complexity of renal handling of drugs within CKD by incorporating physiological changes, as well as the competitive inhibition of uremic toxins and downregulation of metabolic enzymes and transporters [11, 62–65]. The work conducted within this analysis builds upon this foundation and a previously validated CKD parameterization that has incorporated these physiological changes [7]. Successful predictions of exposure for the investigative drugs from real-world clinical trials support the use of this PBPK modeling approach for OAT1/3 substrates.

Estimations of renal drug clearance approximated through creatinine clearance (Cockcroft–Gault) are based on the "intact nephron hypothesis". This theory suggests that the renal elimination processes, glomerular filtration, tubular secretion, and active reabsorption decline proportionally with the progression of CKD [66–68]. In other words, the theory suggests that the decline in CL_R of a drug that undergoes active tubular secretion is similar to one that does not. A recent analysis by Chapron et al. challenged this hypothesis by demonstrating that the method of scaling by GFR was unable to predict CL_R in CKD for half of the investigative drugs that were eliminated by tubular secretion [68], most notably as CKD progressed. Our results confirmed this approach as 58% of CKD simulations failed to meet successful predictions of AUC_∞ using the conventional scaling method, a result that has been demonstrated previously [7]. The conventional scaling method provided reasonable predictions in the early stages of CKD; however, it failed to meet acceptance criteria in more advanced stages (stages 4 and 5). Such a discrepancy was most notably witnessed with meropenem and acyclovir, two molecules with a large contribution of CL_R to total clearance (> 75%) and a large percentage of active tubular secretion accounting for CL_R (> 75%). Therefore, caution should be warranted when incorporating the conventional scaling method to predict PK parameters of molecules with such characteristics in patients with advanced CKD. The results of this analysis highlight that characterization of active tubular secretion by parameterizing the effects of functional changes on OAT within

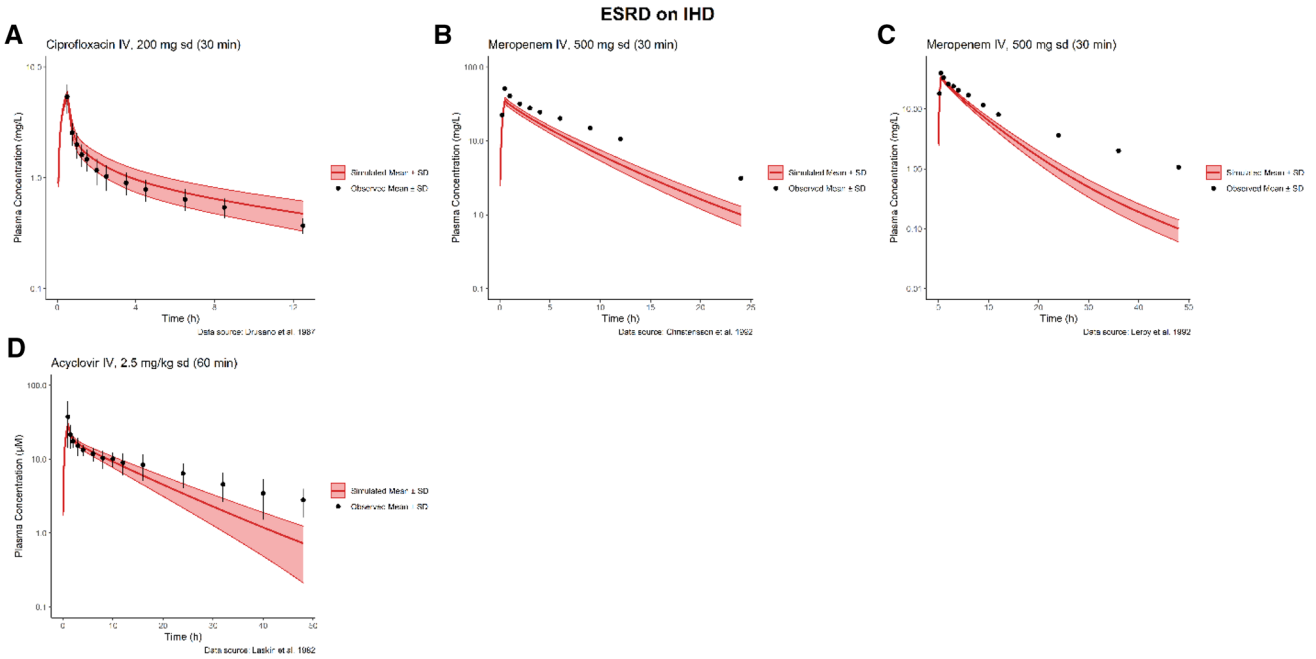

Fig. 6 Simulated chronic kidney disease-physiologically based pharmacokinetic plasma concentration–time profiles compared to observed data for patients with end-stage renal disease undergoing intermittent hemodialysis. Observed data presented as mean (circles) with standard error of the mean (error bars) for each respective study [54, 56, 57, 60]. The red line represents the simulated mean concentration–time profile facilitated by the population chronic kidney disease-physiologically based pharmacokinetic models in PK-Sim, while the shaded region indicates the corresponding standard deviation (SD). Details on the dosing regimen and study populations are shown in the ESM. *IV* intravenous, *sd* single dose

CKD is of the upmost importance for accurately describing the PK within this population.

p-Aminohippuric acid CL_R may be used as an estimator of renal plasma flow because of its high extraction ratio in a healthy kidney, ability for free filtration from plasma, low protein binding, and negligible tubular reabsorption [39, 69–71]. In vitro, OAT1 has been identified as an efficient transporter for PAH [72–74]. Although, additional work has recorded limited and variable affinity of PAH for the OAT3 transporter, it is generally assumed that PAH has a greater affinity for the OAT1 transporter [74, 75]. As such, utilizing PAH as a surrogate for OAT1/3-mediated renal secretion within our unique parameterization across the stages of CKD offers mechanistic and physiologic relevance. It should be noted, all data sets included within the OAT parameterization determined EPAH at steady-state concentrations upon continuous infusion of PAH. This methodology ensures saturation of renal tubules and provides an accurate representation of PAH CL_R [72, 76]. Through investigation of the relationship between EPAH and GFR, we determined that OAT-mediated excretion was reduced by 27–49%, 50–69%, and 70–96% across CKD stages 3, 4, and 5, respectively. Previous reports by Hsueh et al. from an analysis of 18 OAT substrates within CKD determined a median reduction of secretory clearance of 27% and 59% in moderate and severe stages of CKD [10]. Our results coincide with these reported values.

Conclusions in this analysis are in accordance with previous work suggesting that reductions in OAT clearance should occur in addition to impairment of GFR and CL_{NR} processes in PBPK models of severe CKD [11]. However, the work presented here offers several key differences. First, this analysis uniquely incorporated DDI-PBPK modeling using probenecid within our base model construction following a "middle-out" approach to address the knowledge gaps in OAT transporter expression in the kidneys of patients with CKD [4, 35, 62]. DDI-PBPK modeling has served as a valuable tool in drug development to provide mechanistic insight into clinically relevant DDIs [77–80]. Incorporation of probenecid DDI-PBPK model simulations enabled the identification of a unique solution for the contribution of OAT-mediated renal excretion in total CL for each compound. Second, development of an OAT parametrization across stages of CKD through EPAH confirms that reducing CL_R in proportion to GFR is not sufficient to describe the PK of OAT substrates across all stages of CKD. Utilizing this approach increases the generalizability as the OAT-mediated renal excretion may be manipulated to further reflect the degree of renal impairment of the population of interest. Further research is essential to expand upon this analysis

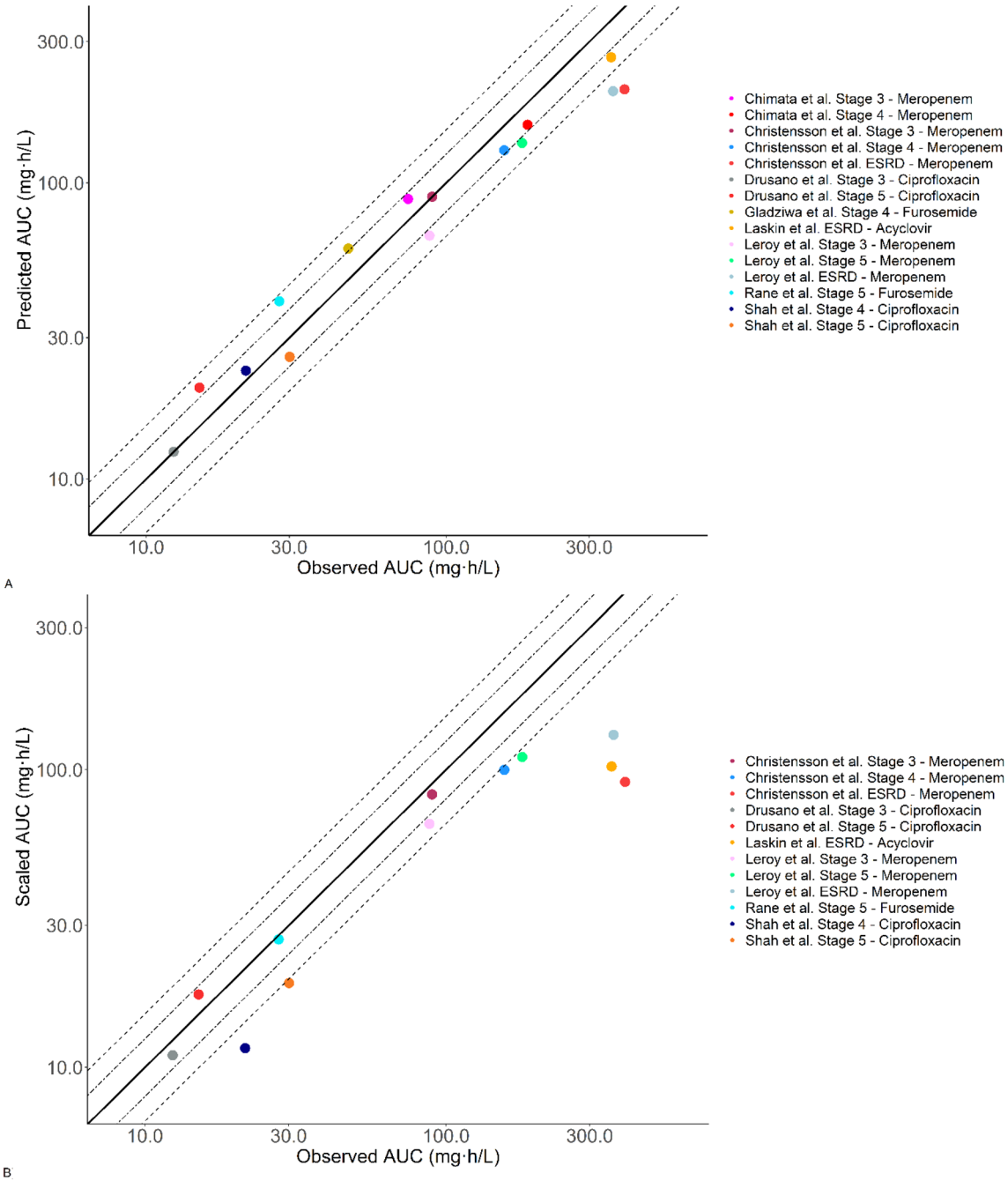

Fig. 7 Predicted vs observed area under the concentration–time curve extrapolated to infinity (AUC_{∞}) of included simulations using chronic kidney disease-physiologically based pharmacokinetic simulations (**A**) in comparison to conventional scaling methods (**B**). The dashed line represents a 1.25-fold error, while the dotted line represents a 1.5-fold error. *AUC* area under the curve, *ESRD* end-stage renal disease

for alternative OAT substrates with varying contributions of tubular secretion on total clearance.

The chronic state of inflammation and uremia throughout CKD has been cited as a contributing factor for the inhibition or downregulation of CL_{NR} processes within this population [63, 64, 81, 82]. Increasing efforts have sought to quantify the decreases in CL_{NR} throughout CKD progression; however, the degree of effect amongst pathways may be quite variable [35, 63, 64]. The four investigative drugs within this analysis undergo different mechanisms of CL_{NR},

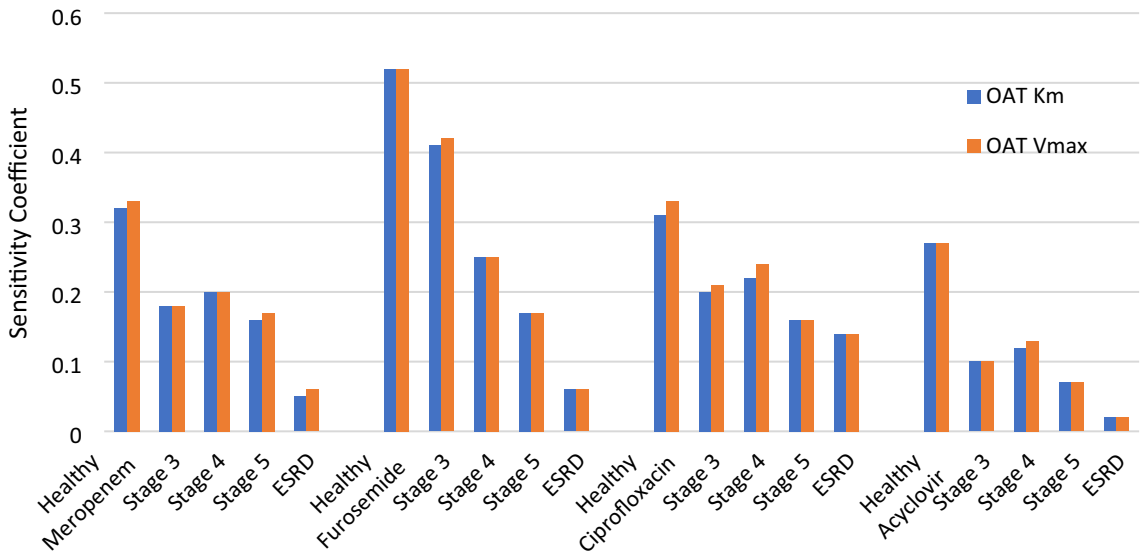

Fig. 8 Local sensitivity analysis for OAT1/3 drug–drug interaction potential for healthy individuals compared with patients with chronic kidney disease for each investigative drug. The OAT transporter Michaelis–Menten constant (K_M) and maximum rate of reaction (V_{max}) were varied by ± 10% to analyze the relative change in area under the concentration–time curve extrapolated to infinity. *ESRD* end-stage renal disease on intermittent hemodialysis

however, all are predominantly renally cleared ($fe_{urine} > 0.5$). As a result, the effects of reduced CL_{NR} on simulated AUC_∞ appears to be minimal. Utilization of these scaling factors enabled accurate predictions of AUC_∞ with the investigative drugs across all stages of CKD; however, further analyses are required to determine the validity in drugs that undergo predominant CL_{NR}. Information on enzyme-specific pathways is preferred where applicable [63, 64].

The analysis is not without limitations. Using EPAH vs eGFR for OAT parameterization allowed us to successfully predict the decline in OAT-mediated secretion throughout CKD. However, as depicted in Fig. 1, there is a paucity of data investigating this relationship in severe CKD. This may have over-predicted the contribution of OAT secretion in stage 5 CKD for patients undergoing IHD between dialysis sessions and could explain the trend to underpredict AUC_∞ for meropenem and acyclovir. Future studies investigating EPAH in severe CKD may enhance the accuracy of model predictions.

Second, the four investigative drugs chosen within this analysis were all administered intravenously. While the findings for renal OAT are generalizable, there are additional uncertain factors that may need to be accounted for when simulating the oral PK of an OAT substrate drug in CKD. Chronic uremia throughout CKD progression may disrupt gastrointestinal physiology, leading to reductions in gastric emptying time and small and large intestinal transit times [83, 84]. Additionally, many OAT substrates such as cephalexin, methotrexate, ciprofloxacin, and rosuvastatin have been documented to also be substrates of the organic anion transporting polypeptide (OATP) family—transporters responsible for the absorption of relevant compounds from the intestinal lumen [23, 85]. Reductions in the uptake of OATP substrates into hepatocytes have been documented in CKD; however, the impact on oral bioavailability remains largely undefined [63, 86–88]. Future research is needed to accurately describe any potential PK changes of orally administered OAT/OATP substrates in patients with CKD.

Third, in the analyses including patients with ESRD undergoing IHD, there was a tendency to over-predict CL_R, resulting in an inability to meet acceptance criteria for two simulations (Fig. 6). It was assumed that apical transporter function on the renal tubule remains largely intact owing to the inability to identify the specific transporter for each molecule and limited data supporting the functionality across CKD [5]. However, several in vivo animal studies suggest that apical transporters may be susceptible to uremic toxin inhibition and/or down-regulation as CKD progresses [88–91]. Contributions of such physiologic changes cannot be discounted within this population and further work is required to provide a more accurate representation of the renal drug handling of OAT substrates in the most severe stages of CKD.

Previous work has identified genetic polymorphisms amongst differing ethnicities that may have the potential to affect OAT activity by reducing the capacity for tubular secretion [92–94]. However, the results of such polymorphisms appear to have a negligible effect on CL_R and tubular secretion in healthy individuals [95]. The observed clinical PK studies in healthy patients and patients with CKD

to which PBPK models were constructed and validated did not report ethnicities of study participants. As a result, differences in physiology and PK based on ethnicities were not considered in the model. Further research is needed to confirm any potential contribution of genetic polymorphisms of OAT activity in those with CKD.

Finally, challenges in model verification were limited because of the lack of available individual subject data within CKD studies. All but one study by Laskin et al. included mean subject PK data used for model comparison (Fig. 2 of the ESM) [60]. However, when comparing a range of exposures within individual-level data, the predicted mean exposure fell within the upper and lower limits (234–498 µmol• h/L). Future work including individual PK data will allow for further assessment of model accuracy. Additionally, the model may be refined upon availability of clinical data to expand with additional compounds, incorporation of OAT polymorphisms [96], or age differences to predict changes in PK for pediatric patients.

Dedicated PK studies in subjects with renal impairment offer many challenges because of the potential for toxic exposures and difficulties in recruitment. There is clear application for this work in drug development, assessing the PK of investigational drugs that are OAT substrates in patients with CKD ahead of clinical trials to assist with dose selection and clinical trial planning. When CKD effects on drug disposition are well characterized, CKD-PBPK models can be used to estimate DDIs in patients with CKD, or even estimate PK parameters across the disease spectrum in different ages, sexes, and body weights that were not tested. There is also potential to supplement the clinical data collected from renal impairment trials so that the results are confirmatory, rather than exploratory. Fewer of these vulnerable subjects will be required to be enrolled in the studies.

5 Conclusions

Use of PBPK modeling within organ impairment to inform dose selection has not been supported with an adequate level of confidence from regulatory agencies such as the US Food and Drug Administration and the European Medicines Agency, especially in more advanced stages [49, 97]. This work builds more evidence toward this end. Utilizing a unique PBPK-DDI model development approach and parameterizing OAT-mediated excretion through EPAH, we were accurately able to predict exposures of four OAT substrates across the stages of CKD. However, the results should be interpreted with caution because of the limited number of drugs investigated, small sample sizes of included studies, and similar PK characteristics between molecules (i.e., OAT substrates with a high contribution of active tubular secretion).

Although further refinement and verification may be needed for oral OAT substrates, the proposed workflow provides a building block towards quantifying the effects of CKD disease progression on CL_R, and more specifically the contribution of OAT-mediated tubular secretion to the elimination of major substrate drugs. The work herein adequately predicts the intravenous PK and renal handling of OAT substrates in patients with CKD but may under-predict concentrations in patients undergoing IHD between dialysis sessions. A quantitative understanding of the reduction in OAT1/3-mediated excretion of drugs in varying stages of renal impairment will contribute to better predictive accuracy for PBPK models in drug development, assisting with clinical trial planning and potentially sparing this population from unnecessary toxic exposures.

Supplementary Information The online version contains supplementary material available at https://doi.org/10.1007/s40262-022-01121-6.

Declarations

Funding No sources of funding were received for the preparation of this article.

Conflicts of interest The authors have no conflicts of interest that are directly relevant to the content of this article.

Ethics approval Not applicable.

Consent to participate Not applicable.

Consent for publication Not applicable.

Availability of data and material Not applicable.

Code availability Not applicable.

Author contributions SD, PM, and AE conceptualized the idea and topic of this article. SD and PM contributed to a healthy adult PBPK model construction of the investigative drugs analyzed within this article. SD conducted the CKD-PBPK simulations and analyzed the results. DH was instrumental in the development and finalization of the OAT parameterization function used throughout the CKD-PBPK simulations. Contributions from PM were final as of 11 June, 2021. Preparation of the final manuscript was conducted by SD. The final version of manuscript was reviewed by all authors.

References

1. Purcell CA, Abebe M, Adebayo OM, et al. Global, regional, and national burden of chronic kidney disease, 1990–2017: a systematic analysis for the global burden of disease study 2017. Lancet. 2020;395(10225):709–33. https://doi.org/10.1016/S0140-6736(20)30045-3.
2. KDIGO (Kidney Disease: Improving Global Outcomes). Acute kidney injury. 2012. https://kdigo.org/wp-content/uploads/2016/10/KDIGO-2012-AKI-Guideline-English.pdf. Accessed 18 Mar 2022.

3. Manley HJ, Cannella CA, Bailie GR, St Peter WL. Medication-related problems in ambulatory hemodialysis patients: a pooled analysis. Am J Kidney Dis. 2005;46(4):669–80. https://doi.org/10.1053/j.ajkd.2005.07.001.
4. Morrissey KM, Stocker SL, Wittwer MB, Xu L, Giacomini KM. Renal transporters in drug development. Annu Rev Pharmacol Toxicol. 2013;53:503–29. https://doi.org/10.1146/annurev-pharmtox-011112-140317.
5. Torres AM, Dnyanmote AV, Granados JC, Nigam SK. Renal and non-renal response of ABC and SLC transporters in chronic kidney disease. Expert Opin Drug Metab Toxicol. 2021;17(5):515–42. https://doi.org/10.1080/17425255.2021.1899159.
6. Cheung KWK, Hsueh C, Zhao P, et al. The effect of uremic solutes on the organic cation transporter 2. J Pharm Sci. 2017;106(9):2551–7. https://doi.org/10.1016/j.xphs.2017.04.076.
7. Malik PRV, Yeung CHT, Ismaeil S, Advani U, Djie S, Edginton AN. A physiological approach to pharmacokinetics in chronic kidney disease. J Clin Pharmacol. 2020;60(S1):S52-62. https://doi.org/10.1002/jcph.1713.
8. Droździk M, Oswald S, Droździk A. Impact of kidney dysfunction on hepatic and intestinal drug transporters. Biomed Pharmacother. 2021;143: 112125. https://doi.org/10.1016/j.biopha.2021.112125.
9. Masereeuw R, Mutsaers HAM, Toyohara T, et al. The kidney and uremic toxin removal: glomerulus or tubule? Semin Nephrol. 2014;34(2):191–208. https://doi.org/10.1016/j.semnephrol.2014.02.010.
10. Hsueh C, Yoshida K, Zhao P, et al. Identification and quantitative assessment of uremic solutes as inhibitors of renal organic anion transporters, OAT1 and OAT3. Mol Pharm. 2016;13(9):3130–40. https://doi.org/10.1021/acs.molpharmaceut.6b00332.
11. Hsueh C, Hsu V, Zhao P, Zhang L, Giacomini KM, Huang S. PBPK modeling of the effect of reduced kidney function on the pharmacokinetics of drugs excreted renally by organic anion transporters. Clin Pharmacol Ther. 2018;103(3):485–92. https://doi.org/10.1002/cpt.750.
12. Willmann S, Höhn K, Edginton A, et al. Development of a physiology-based whole-body population model for assessing the influence of individual variability on the pharmacokinetics of drugs. J Pharmacokinet Pharmacodyn. 2007;34(3):401–31. https://doi.org/10.1007/s10928-007-9053-5.
13. Schlender J, Meyer M, Thelen K, et al. Development of a whole-body physiologically based pharmacokinetic approach to assess the pharmacokinetics of drugs in elderly individuals. Clin Pharmacokinet. 2016;55(12):1573–89. https://doi.org/10.1007/s40262-016-0422-3.
14. Schlender J, Teutonico D, Coboeken K, et al. A physiologically-based pharmacokinetic model to describe ciprofloxacin pharmacokinetics over the entire span of life. Clin Pharmacokinet. 2018;57(12):1613–34. https://doi.org/10.1007/s40262-018-0661-6.
15. Britz H, Hanke N, Taub ME, et al. Physiologically based pharmacokinetic models of probenecid and furosemide to predict transporter mediated drug-drug interactions. Pharm Res. 2020;37(12):250. https://doi.org/10.1007/s11095-020-02964-z.
16. Mouton JW, van den Anker JN. Meropenem clinical pharmacokinetics. Clin Pharmacokinet. 1995;28(4):275–86. https://doi.org/10.2165/00003088-199528040-00002.
17. Merrem (meropenem). Prescribing information. Boucherville: Sandoz Canada Inc.; 2017.
18. Arnal J, Gonzalez-Alvarez I, Bermejo M, et al. Biowaiver monographs for immediate release solid oral dosage forms: aciclovir. J Pharm Sci. 2008;97(12):5061–73. https://doi.org/10.1002/jps.21392.
19. DrugBank. Meropenem. https://go.drugbank.com/drugs/DB00760. Accessed 18 Mar 2022.
20. Jaehde U, Sörgel F, Reiter A, Sigl G, Naber KG, Schunack W. Effect of probenecid on the distribution and elimination of ciprofloxacin in humans. Clin Pharmacol Ther. 1995;58(5):532–41.
21. Bax RP, Bastain W, Featherstone A, Wilkinson DM, Hutchison M, Haworth SJ. The pharmacokinetics of meropenem in volunteers. J Antimicrob Chemother. 1989;24(Suppl A):311–20.
22. de Miranda P, Good SS, Laskin OL, Krasny HC, Connor JD, Lietman PS. Disposition of intravenous radioactive acyclovir. Clin Pharmacol Ther. 1981;30(5):662–72.
23. Momper JD, Tsunoda SM, Ma JD. Evaluation of proposed in vivo probe substrates and inhibitors for phenotyping transporter activity in humans. J Clin Pharmacol. 2016;56(Suppl. 7):82. https://doi.org/10.1002/jcph.736.
24. Shibayama T, Sugiyama D, Kamiyama E, Tokui T, Hirota T, Ikeda T. Characterization of CS-023 (RO4908463), a novel parenteral carbapenem antibiotic, and meropenem as substrates of human renal transporters. Drug Metab Pharmacokinet. 2007;22(1):41–7. https://doi.org/10.2133/dmpk.22.41.
25. Ivanyuk A, Livio F, Biollaz J, Buclin T. Renal drug transporters and drug interactions. Clin Pharmacokinet. 2017;56(8):825–92. https://doi.org/10.1007/s40262-017-0506-8.
26. Scotcher D, Billington S, Brown J, et al. Microsomal and cytosolic scaling factors in dog and human kidney cortex and application for in vitro-in vivo extrapolation of renal metabolic clearance. Drug Metab Dispos. 2017;45(5):556–8. https://doi.org/10.1124/dmd.117.075242.
27. Prasad B, Johnson K, Billington S, et al. Abundance of drug transporters in the human kidney cortex as quantified by quantitative targeted proteomics. Drug Metab Dispos. 2016;44(12):1920–4. https://doi.org/10.1124/dmd.116.072066.
28. Uchino H, Tamai I, Yabuuchi H, et al. Faropenem transport across the renal epithelial luminal membrane via inorganic phosphate transporter Npt1. Antimicrob Agents Chemother. 2000;44(3):574–7.
29. Willmann S, Lippert J, Schmitt W. From physicochemistry to absorption and distribution: predictive mechanistic modelling and computational tools. Expert Opin Drug Metab Toxicol. 2005;1(1):159–68. https://doi.org/10.1517/17425255.1.1.159.
30. Rodgers T, Leahy D, Rowland M. Physiologically based pharmacokinetic modeling 1: predicting the tissue distribution of moderate-to-strong bases. J Pharm Sci. 2005;94(6):1259–76. https://doi.org/10.1002/jps.20322.
31. Rodgers T, Rowland M. Physiologically based pharmacokinetic modelling 2: predicting the tissue distribution of acids, very weak bases, neutrals and zwitterions. J Pharm Sci. 2006;95(6):1238–57. https://doi.org/10.1002/jps.20502.
32. Hsu V, de Vieira LT, Manuela ZP, et al. Towards quantitation of the effects of renal impairment and probenecid inhibition on kidney uptake and efflux transporters, using physiologically based pharmacokinetic modelling and simulations. Clin Pharmacokinet. 2014;53(3):283–93. https://doi.org/10.1007/s40262-013-0117-y.
33. Doki K, Neuhoff S, Rostami-Hodjegan A, Homma M. Assessing potential drug–drug interactions between dabigatran etexilate and P-glycoprotein inhibitor in renal impairment populations using physiologically based pharmacokinetic modeling. CPT Pharmacomet Syst Pharmacol. 2019;8(2):118–26.
34. Tsamandouras N, Rostami-Hodjegan A, Aarons L. Combining the 'bottom up' and 'top down' approaches in pharmacokinetic modelling: fitting PBPK models to observed clinical data. Br J Clin Pharmacol. 2015;79(1):48–55.
35. Sayama H, Takubo H, Komura H, Kogayu M, Iwaki M. Application of a physiologically based pharmacokinetic model informed by a top-down approach for the prediction of pharmacokinetics in chronic kidney disease patients. AAPS J. 2014;16(5):1018–28. https://doi.org/10.1208/s12248-014-9626-3.

36. Basit A, Radi Z, Vaidya VS, Karasu M, Prasad B. Kidney cortical transporter expression across species using quantitative proteomics. Drug Metab Dispos. 2019;47(8):802–8. https://doi.org/10.1124/dmd.119.086579.
37. Mahmood I, Tegenge MA. A comparative study between allometric scaling and physiologically based pharmacokinetic modeling for the prediction of drug clearance from neonates to adolescents. J Clin Pharmacol. 2019;59(2):189–97. https://doi.org/10.1002/jcph.1310.
38. Smith HW, Finkelstein N, Aliminosa L, Crawford B, Graber M. The renal clearances of substituted hippuric acid derivatives and other aromatic acids in dog and man. J Clin Investig. 1945;24(3):388–404. https://doi.org/10.1172/JCI101618.
39. Nigam SK, Bush KT, Martovetsky G, et al. The organic anion transporter (OAT) family: a systems biology perspective. Physiol Rev. 2015;95(1):83–123. https://doi.org/10.1152/physrev.00025.2013.
40. Ullrich KJ, Rumrich G. Renal transport mechanisms for xenobiotics: chemicals and drugs. Clin Investig. 1993;71(10):843–8. https://doi.org/10.1007/BF00190334.
41. Dantzler WH, Wright SH. The molecular and cellular physiology of basolateral organic anion transport in mammalian renal tubules. Biochim Biophys Acta. 2003;1618(2):185–93. https://doi.org/10.1016/j.bbamem.2003.08.015.
42. Battilana C, Zhang HP, Olshen RA, Wexler L, Myers BD. PAH extraction and estimation of plasma flow in diseased human kidneys. Am J Physiol. 1991;261(4 Pt 2):726. https://doi.org/10.1152/ajprenal.1991.261.4.F726.
43. Bergstrom J, Bucht H, Ek J, Josephson B, Sundell H, Werko L. The renal extraction of para-aminohippurate in normal persons and in patients with diseased kidneys. Scand J Clin Lab Investig. 1959;11:361–75. https://doi.org/10.3109/00365515909060466.
44. Bradley SE, Bradley GP, Tyson CJ, Curry JJ, Blake WD. Renal function in renal diseases. Am J Med. 1950;9(6):766–98. https://doi.org/10.1016/0002-9343(50)90292-0.
45. Brodwall EK. Renal extraction of PAH in renal disease. Scand J Clin Lab Investig. 1964;16(1):12–20. https://doi.org/10.3109/00365516409060477.
46. Josephson B, Bucht H, Ek J, Werko L. Renal extraction, its depression, and the tubular storage of p-aminohippuric acid (PAH) in the healthy and in the diseased human kidney. Scand J Clin Lab Investig. 1952;4(1):1–14. https://doi.org/10.3109/00365515209060626.
47. Cargill WH. The measurement of glomerular and tubular plasma flow in the normal and diseased human kidney. J Clin Investig. 1949;28(3):533–8.
48. Zhang Y, Zhang L, Abraham S, et al. Assessment of the impact of renal impairment on systemic exposure of new molecular entities: evaluation of recent new drug applications. Clin Pharmacol Ther. 2009;85(3):305–11. https://doi.org/10.1038/clpt.2008.208.
49. Zhang L, Xu N, Xiao S, et al. Regulatory perspectives on designing pharmacokinetic studies and optimizing labeling recommendations for patients with chronic kidney disease. J Clin Pharmacol. 2012;52(1 Suppl.):79S-90S. https://doi.org/10.1177/0091270011415410.
50. Yoshida K, Sun B, Zhang L, et al. Systematic and quantitative assessment of the effect of chronic kidney disease on CYP2D6 and CYP3A4/5. Clin Pharmacol Ther. 2016;100(1):75–87. https://doi.org/10.1002/cpt.337.
51. Laskin OL, de Miranda P, King DH, et al. Effects of probenecid on the pharmacokinetics and elimination of acyclovir in humans. Antimicrob Agents Chemother. 1982;21(5):804–7.
52. Wiebe ST, Giessmann T, Hohl K, et al. Validation of a drug transporter probe cocktail using the prototypical inhibitors rifampin, probenecid, verapamil, and cimetidine. Clin Pharmacokinet. 2020;59(12):1627–39. https://doi.org/10.1007/s40262-020-00907-w.
53. Chimata M, Nagase M, Suzuki Y, Shimomura M, Kakuta S. Pharmacokinetics of meropenem in patients with various degrees of renal function, including patients with end-stage renal disease. Antimicrob Agents Chemother. 1993;37(2):229–33.
54. Drusano GL, Weir M, Forrest A, Plaisance K, Emm T, Standiford HC. Pharmacokinetics of intravenously administered ciprofloxacin in patients with various degrees of renal function. Antimicrob Agents Chemother. 1987;31(6):860–4. https://doi.org/10.1128/AAC.31.6.860.
55. Shah A, Lettieri J, Blum R, Millikin S, Sica D, Heller AH. Pharmacokinetics of intravenous ciprofloxacin in normal and renally impaired subjects. J Antimicrob Chemother. 1996;38(1):103–16. https://doi.org/10.1093/jac/38.1.103.
56. Christensson BA, Nilsson-Ehle I, Hutchison M, Haworth SJ, Oqvist B, Norrby SR. Pharmacokinetics of meropenem in subjects with various degrees of renal impairment. Antimicrob Agents Chemother. 1992;36(7):1532–7. https://doi.org/10.1128/AAC.36.7.1532.
57. Leroy A, Fillastre JP, Etienne I, Borsa-Lebás F, Humbert G. Pharmacokinetics of meropenem in subjects with renal insufficiency. Eur J Clin Pharmacol. 1992;42(5):535–8. https://doi.org/10.1007/BF00314864.
58. Gladziwa U, Böhm R, Klotz U, et al. Pharmacokinetics of furosemide in patients with chronic renal failure. Drug Investig. 1993;6:137–43. https://doi.org/10.1007/BF03259733.
59. Rane A, Villeneuve JP, Stone WJ, Nies AS, Wilkinson GR, Branch RA. Plasma binding and disposition of furosemide in the nephrotic syndrome and in uremia. Clin Pharmacol Ther. 1978;24(2):199–207. https://doi.org/10.1002/cpt1978242199.
60. Laskin OL, Longstreth JA, Whelton A, et al. Acyclovir kinetics in end-stage renal disease. Clin Pharmacol Ther. 1982;31(5):594–601. https://doi.org/10.1038/clpt.1982.83.
61. Bush KT, Singh P, Nigam SK. Gut-derived uremic toxin handling in vivo requires OAT-mediated tubular secretion in chronic kidney disease. JCI Insight. 2020;9(5): e133817. https://doi.org/10.1172/jci.insight.133817.
62. Rowland Yeo K, Aarabi M, Jamei M, Rostami-Hodjegan A. Modeling and predicting drug pharmacokinetics in patients with renal impairment. Expert Rev Clin Pharmacol. 2011;4(2):261–74. https://doi.org/10.1586/ecp.10.143.
63. Tan M, Yoshida K, Zhao P, et al. Effect of chronic kidney disease on nonrenal elimination pathways: a systematic assessment of CYP1A2, CYP2C8, CYP2C9, CYP2C19, and OATP. Clin Pharmacol Ther. 2018;103(5):854–67. https://doi.org/10.1002/cpt.807.
64. Tan M, Zhao P, Zhang L, et al. Use of physiologically based pharmacokinetic modeling to evaluate the effect of chronic kidney disease on the disposition of hepatic CYP2C8 and OATP1B drug substrates. Clin Pharmacol Ther. 2019;105(3):719–29. https://doi.org/10.1002/cpt.1205.
65. Follman KE, Morris ME. Prediction of the effects of renal impairment on clearance for organic cation drugs that undergo renal secretion: a simulation-based study. Drug Metab Dispos. 2018;46(5):758–69. https://doi.org/10.1124/dmd.117.079558.
66. Bricker NS. On the meaning of the intact nephron hypothesis. Am J Med. 1969;46(1):1–11. https://doi.org/10.1016/0002-9343(69)90053-9.
67. Dettli L. Drug dosage in renal disease. Clin Pharmacokinet. 1976;1(2):126–34. https://doi.org/10.2165/00003088-197601020-00004.
68. Chapron A, Shen DD, Kestenbaum BR, Robinson-Cohen C, Himmelfarb J, Yeung CK. Does secretory clearance follow glomerular filtration rate in chronic kidney diseases? Reconsidering the intact nephron hypothesis. Clin Transl Sci. 2017;10(5):395–403. https://doi.org/10.1111/cts.12481.

69. Momper JD, Yang J, Gockenbach M, Vaida F, Nigam SK. Dynamics of organic anion transporter-mediated tubular secretion during postnatal human kidney development and maturation. Clin J Am Soc Nephrol. 2019;14(4):540–8. https://doi.org/10.2215/CJN.10350818.
70. Toto RD. Conventional measurement of renal function utilizing serum creatinine, creatinine clearance, inulin and para-aminohippuric acid clearance. Curr Opin Nephrol Hypertens. 1995;4(6):505–9. https://doi.org/10.1097/00041552-199511000-00009.
71. Dowling TC, Frye RF, Fraley DS, Matzke GR. Characterization of tubular functional capacity in humans using para-aminohippurate and famotidine. Kidney Int. 2001;59(1):295–303. https://doi.org/10.1046/j.1523-1755.2001.00491.x.
72. Sweet DH, Miller DS, Pritchard JB, Fujiwara Y, Beier DR, Nigam SK. Impaired organic anion transport in kidney and choroid plexus of organic anion transporter 3 (Oat3 (Slc22a8)) knockout mice. J Biol Chem. 2002;277(30):26934–43. https://doi.org/10.1074/jbc.M203803200.
73. Eraly SA, Vallon V, Vaughn DA, et al. Decreased renal organic anion secretion and plasma accumulation of endogenous organic anions in OAT1 knock-out mice. J Biol Chem. 2006;281(8):5072–83. https://doi.org/10.1074/jbc.M508050200.
74. Rizwan AN, Krick W, Burckhardt G. The chloride dependence of the human organic anion transporter 1 (hOAT1) is blunted by mutation of a single amino acid. J Biol Chem. 2007;282(18):13402–9. https://doi.org/10.1074/jbc.M609849200.
75. Burckhardt G, Bahn A, Wolff NA. Molecular physiology of renal p-aminohippurate secretion. News Physiol Sci. 2001;16:114–8. https://doi.org/10.1152/physiologyonline.2001.16.3.114.
76. Schumann L, Wüstenberg PW. An improved method to determine renal function using inulin and p-aminohippurate (PAH) steady-state kinetic modeling. Clin Nephrol. 1990;33(1):35–40.
77. Hanke N, Frechen S, Moj D, et al. PBPK models for CYP3A4 and p-gp DDI prediction: a modeling network of rifampicin, itraconazole, clarithromycin, midazolam, alfentanil, and digoxin. CPT Pharmacomet Syst Pharmacol. 2018;7(10):647–59. https://doi.org/10.1002/psp4.12343.
78. Center for Drug Evaluation and Research. Clinical pharmacology and biopharmaceutics review: olumiant. Published December 2017. Baricitinib. https://www.accessdata.fda.gov/drugsatfda_docs/nda/2018/207924Orig1s000ClinPharmR.pdf. Accessed Sep 2021.
79. Posada MM, Bacon JA, Schneck KB, et al. Prediction of renal transporter mediated drug–drug interactions for pemetrexed using physiologically based pharmacokinetic modeling. Drug Metab Dispos. 2015;43(3):325–34. https://doi.org/10.1124/dmd.114.059618.
80. Salerno SN, Carreño FO, Edginton AN, Cohen-Wolkowiez M, Gonzalez D. Leveraging physiologically based pharmacokinetic modeling and experimental data to guide dosing modification of CYP3A-mediated drug-drug interactions in the pediatric population. Drug Metab Dispos. 2021;49(9):844–55. https://doi.org/10.1124/dmd.120.000318.
81. Nolin TD, Frye RF, Matzke GR. Hepatic drug metabolism and transport in patients with kidney disease. Am J Kidney Dis. 2003;42(5):906–25. https://doi.org/10.1016/j.ajkd.2003.07.019.
82. Decker BS, O'Neill KD, Chambers MA, et al. Hemodialysis does not alter in vitro hepatic CYP3A4 and CYP2D6 metabolic activity in uremic serum. Clin Pharmacol. 2013;5:193–9. https://doi.org/10.2147/CPAA.S54381.
83. Hirako M, Kamiya T, Misu N, et al. Impaired gastric motility and its relationship to gastrointestinal symptoms in patients with chronic renal failure. J Gastroenterol. 2005;40(12):1116–22. https://doi.org/10.1007/s00535-005-1709-6.
84. Vaziri ND, Yuan J, Nazertehrani S, Ni Z, Liu S. Chronic kidney disease causes disruption of gastric and small intestinal epithelial tight junctions. Am J Nephrol. 2013;38(2):99–103. https://doi.org/10.1159/000353764.
85. Shitara Y, Maeda K, Ikejiri K, Yoshida K, Horie T, Sugiyama Y. Clinical significance of organic anion transporting polypeptides (OATPs) in drug disposition: their roles in hepatic clearance and intestinal absorption. Biopharm Drug Dispos. 2013;34(1):45–78. https://doi.org/10.1002/bdd.1823.
86. Nolin TD, Frye RF, Le P, et al. ESRD impairs nonrenal clearance of fexodenadine but not midazolam. J Am Soc Nephrol. 2009;20(10):2269–76. https://doi.org/10.1681/ASN.2009010082.
87. Thomson BKA, Nolin TD, Velenosi TJ, et al. Effect of CKD and dialysis modality on exposure to drugs cleared by nonrenal mechanisms. Am J Kidney Dis. 2015;65(4):574–82. https://doi.org/10.1053/j.ajkd.2014.09.015.
88. Naud J, Michaud J, Beauchemin S, et al. Effects of chronic renal failure on kidney drug transporters and cytochrome P450 in rats. Drug Metab Dispos. 2011;39(8):1363–9. https://doi.org/10.1124/dmd.111.039115.
89. Torres AM, Laughlin MM, Muller A, Brandoni A, Anzai N, Endou H. Altered renal elimination of organic anions in rats with chronic renal failure. Biochim Biophys Acta. 2005;1740(1):29–37. https://doi.org/10.1016/j.bbadis.2005.03.002.
90. Deguchi T, Takemoto M, Uehara N, Lindup WE, Suenaga A, Otagiri M. Renal clearance of endogenous hippurate correlates with expression levels of renal organic anion transporters in uremic rats. J Pharmacol Exp Ther. 2005;314(2):932–8. https://doi.org/10.1124/jpet.105.085613.
91. Nishihara K, Masuda S, Ji L, Katsura T, Inui KI. Pharmacokinetic significance of luminal multidrug and toxin extrusion 1 in chronic renal failure rats. Biochem Pharmacol. 2007;73(9):1482–90. https://doi.org/10.1016/j.bcp.2006.12.034.
92. Xu G, Bhatnagar V, Wen B, Hamilton BA, Early SA, Nigam SK. Analyses of coding region polymorphisms in apical and basolateral human organic anion transporter (OAT) genes [OAT1 (NKT), OAT2, OAT3, OAT4, URAT (RST)]. Kidney Int. 2005;68(4):1491–9.
93. Stephens JC, Schneider JA, Tanguay DA, et al. Haplotype variation and linkage disequilibrium in 313 human genes. Science. 2001;293(5529):489–93.
94. Marzolini C, Tirona RG, Kim RB. Pharmacogenomics of the OATP and OAT families. Pharmacogenomics. 2004;5(3):273–82.
95. Nishizato Y, Ieiri I, Suzuki H, et al. Polymorphisms of OATP-C (SLC21A6) and OAT3 (SLC22A8) genes: consequences of pravastatin pharmacokinetics. Clin Pharmacol Ther. 2003;73(6):554–65.
96. Lozano E, Briz O, Macias RIR, et al. Genetic heterogeneity of SLC22 family of transporters in drug disposition. J Pers Med. 2018;8(2):14. https://doi.org/10.3390/jpm8020014.
97. Wagner C, Zhao P, Pan Y, et al. Application of physiologically based pharmacokinetic (PBPK) modeling to support dose selection: report of an FDA public workshop on PBPK. CPT Pharmacomet Syst Pharmacol. 2015;4(4):226–30. https://doi.org/10.1002/psp4.33.